23rd International Congress on Sound & Vibration
Athens, Greece 10-14 July 2016
ICSV23

NUMERICAL PREDICTION OF THERMOACOUSTIC INSTABILITIES WITH A V-FLAME

Wei Na, Gunilla Efraimsson and Susann Boij
Department of Aeronautical and Vehicle Engineering
Royal Institute of Technology, Stockholm, Sweden
Linné FLOW Centre
email: wein@kth.se

In this paper, results from a numerical solver for the Helmholtz equation using the Finite Element Method (FEM) for predicting thermoacoustic instabilities are presented. The one-dimensional n-τ flame model, which is governed by an interaction index n and a time-delay τ as well as a Flame transfer function (FTF) is used for flame source term.

We show results for the validation of the numerical solver for the Rijke tube benchmark case with the variation of n and τ in the one-dimensional n-τ model. Thereafter, thermoacoustic instabilities for a V-flame are predicted, for a typical configuration of a dump combustor - a tube with an area expansion. This is a more realistic test case, since a bluff-body flame holder is often used in combustors, where a V-flame will be generated and anchored to the rod. Usually, the V-flame is more susceptible to thermoacoustic instabilities. In the paper, the eigenfrequencies, as well as the acoustic pressure perturbations are presented as numerical results.

1. Introduction

Often the unsteady heat release rate in a combustor is due to the equivalence ratio fluctuations, flow turbulence, flow instabilities, which will lead to the generation of the sound wave. In turn, the flame is perturbed by sound waves which are due to reflections at obstacles or area changes. Once the sound wave is in phase of the pressure oscillations, combustion instabilities can grow, resulting in a big structural damage in combustors.

The aim of the paper is to describe and evaluate an efficient and accurate numerical tool to predict thermoacoustic instabilities in combustors. As a validation case, results for the Rijke tube test case with a planar and fixed flame are presented in the paper. Afterwards, a more realistic flame transfer function (FTF) has been introduced into the numerical solver to predict the thermoacoustic instabilities for a V-flame. In the simulations, the finite element method (FEM) has been used. The sensitivity of the solver is studied via variation of the governing parameters of the flame model.

2. Numerical Methodology

2.1 The Inhomogeneous Helmholtz Equation

For low Mach number (Ma < 0.05) and constant mean pressure flows, the wave equation incorporating a heat release source term in the time domain models the interaction between the flame and the acoustics. We have

$$\nabla \cdot (\bar{c}^2 \nabla p') - \frac{\partial^2 p'}{\partial t^2} = -(\gamma - 1)\frac{\partial \dot{q}'}{\partial t} \tag{1}$$

where primed and over-bared variables stand for the thermo-acoustic perturbation and mean variables, respectively. p, c and $\dot{q}'$ stand for the pressure, sound speed and the heat release rate per volume per unit time. γ is the specific heat ratio and has been assumed to be constant in the derivation. Since thermo-acoustic instabilities usually exhibit in the low/medium frequencies, viscosity as well as thermo-diffusivity may be neglected [1].

Introducting the harmonic variation in time $\phi' = \mathbb{R}\{\hat{\phi}(x)exp(-i\omega t)\}$, Eq.(1) becomes

$$\nabla \cdot (\bar{c}^2 \nabla \hat{p}) + \omega^2 \hat{p} = i\omega(\gamma - 1)\hat{q} \tag{2}$$

The heat release fluctuation $\hat{q}$ is required to close the Eq.(2. For the prediction of thermo-acoustic instabilities the modelling of the unsteady behaviour of the flame is a challenging task. In general, the modelling of flame is usually describing the relation between the unsteady heat release rate and velocity or equivalence ratio fluctuations. Based on this, several models have been proposed, such as describing the response of conical or V-shaped laminar flame [2],[3], and the effect of equivalence ratio fluctuations [4],[5]. A flame transfer function or an analytical model are the common ways to model the heat release fluctuation.

2.2 One-dimentional flame n-τ model

The most famous flame model, is a so-called n-τ model [6]. The n-τ model is essentially a one-dimensional model which links the global heat release at time t to a time lagged acoustic velocity at an reference position. The Eq.(3) represents a compact flame model

$$\dot{Q}'(t) = n\frac{\bar{\dot{Q}}}{\bar{u}_b} u'_i(x_{ref}, t - \tau) n_{ref} \tag{3}$$

where $\dot{Q}'(t)$ is the global fluctuating heat release rate, $\bar{\dot{Q}}$ is its mean counterpart, $\bar{u}_b$ is the bulk velocity at the reference location and u'_i is the acoustic velocity at the reference location x_{ref} and the direction n_{ref}. The factor n governs the strength of the flame response and is called the infection index, τ describes the time lag and controls the phase between acoustic pressure and unsteady heat release rate of the flame and thus the sign of the Rayleigh integral.

However, the compactness assumption is not always fulfilled in the modern gas turbines where the heat release is spatially distributed. In such cases, the compact n-τ model of Eq.(3) can be reformulated to relate the local heat release fluctuations to a velocity fluctuation at the reference location

$$\dot{q}'(x,t) = n_l(x)\frac{\bar{\dot{q}}}{\bar{u}_b} u'(x_{ref}, t - \tau(x)) n_{ref}. \tag{4}$$

Here $\dot{q}'$ is the local unsteady heat release rate per unit volume, $\bar{\dot{q}}$ is the local mean heat release rate per unit volume and $n_l(x)$ is the local interaction index spatially distributed in the flame zone. In frequency domain, Eq.(4) is

$$\hat{q}(x) = n_l(x)\frac{\bar{q}}{\bar{u}_b} e^{i\omega\tau(x)} \hat{u}(x_{ref}) n_{ref} \tag{5}$$

where the acoustic velocity can be replaced by the pressure gradient $i\omega\bar{\rho}\hat{u} = \nabla\hat{p}$ if he zero Mach number assumption is made.

Inserting the flame $n - \tau$ model into Eq. (2), the Helmholtz equation in combination of the $n - \tau$ model is obtained as Eq. (6):

$$\nabla \cdot (\bar{c}^2 \nabla \hat{p}) + \omega^2 \hat{p} = \frac{(\gamma - 1)\bar{q}(x)}{\bar{\rho}(x_{ref})\bar{u}(x_{ref}) \cdot n_{ref}} n_l(x) e^{i\omega\tau(x)} \nabla\hat{p} \cdot n_{ref}(x_{ref}) \tag{6}$$

In the present work, the inhomogeneous Helmholtz equation in combination of the one-dimensional flame $n - \tau$ model as Eq.(6) is discretized using the Finite Element Method and solved by an iterative eigenvalue solver, similar to what is described in [1]. The numerical results by solving Eq.(6) is verified in the Section. 3 for the Rijke tube benchmark case.

2.3 A general flame transfer function

To be more general, a flame transfer function (FTF) is usually used to describe the heat release fluctuation, $\hat{q}$. In its simplest form, the FTF only depends on the frequency and links the ratio between the Fourier transforms of the unsteady heat release rate fluctuations $\hat{\dot{Q}}$ and acoustic velocity fluctuations $\hat{u}$ as [7]

$$F(\omega) = G(\omega)e^{i\omega\tau} = \frac{\hat{\dot{Q}}(\omega)/\bar{\dot{Q}}}{\hat{u}/\bar{u}} \tag{7}$$

Here $\omega = 2\pi f$ stands for the angular frequency of the perturbation, G is the global gain and τ is a time lag. Further, $\bar{\dot{Q}}$ and $\bar{u}$ denote a mean heat release and velocity at the reference location.

The FTF can be either measured or modelled theoretically or numerically. The flame $n-\tau$ model as Eq. (5) can be also represented as a FTF. Naturally, a FTF can be used in numerical simulations. However, in order to account for a FTF, a local flame describing function is required to be included, which can relate the local heat release fluctuation $\hat{\dot{q}}$ to the acoustic velocity at the reference location and reference direction $\hat{u}_{ref} \cdot n_{ref}$ as

$$F_{loc}(x,\omega) = G_{loc}(x,\omega)e^{i\phi_{loc}(x,\omega)} = \frac{\hat{q}(x)/\bar{q}(x_{ref})}{\hat{u}(x_{ref})/\bar{u}(x_{ref}) \cdot n_{ref}} \tag{8}$$

where G_{loc} and ϕ_{loc} represent the local gain the local phase lag, respectively.

By inserting the $\hat{q}$ into the Eq. (2), the inhomogeneous equation in combination of the FTF is obtain as

$$\nabla \cdot (\bar{c}^2 \nabla \hat{p}) + \omega^2 \hat{p} = \frac{(\gamma-1)\bar{q}(x)}{\bar{\rho}(x_{ref})\bar{u}(x_{ref}) \cdot n_{ref}} G_{loc}(x,\omega)\nabla\hat{p} \cdot n_{ref} \cdot e^{i\phi_{loc}(x,\omega)} \tag{9}$$

In Section 4, Eq.(9) is solved numerically using the Finite Element Method together with an iterative eigenvalue solver for a V-flame in a dump combustor.

3. A validation case - the Rijke tube

In this section, the thermo-acoustic instabilities of the Rijke tube under the assumption of low Mach number are calculated. “Passive flame” refers to the case where only the temperature variation without any unsteady flame effect is taken into account , while “active flame” refers to the case in which the unsteady effects of the flame is modelled by the $n-\tau$ model presented in the Section 2.2.

The configuration for the Rijke tube consists of a duct of length $L = 0.5m$ and a constant cross section where the cool gas is separated from the hot gas by a flame of the thickness $\delta = 0.005m$ located at the middle of the duct as is shown in Fig. 3. The temperature T_1 before and T_2 after the flame is 300K and 1200K, respectively, which yields that the cool-to-hot temperature ratio is $T_2/T_1 = 4$. In this numerical case, the acoustic velocity is zero at the inlet, top wall and the bottom wall ($\hat{u} \cdot n = 0$). Moreover, the pressure is fixed at the outlet ($\hat{p} = 0$)[8].

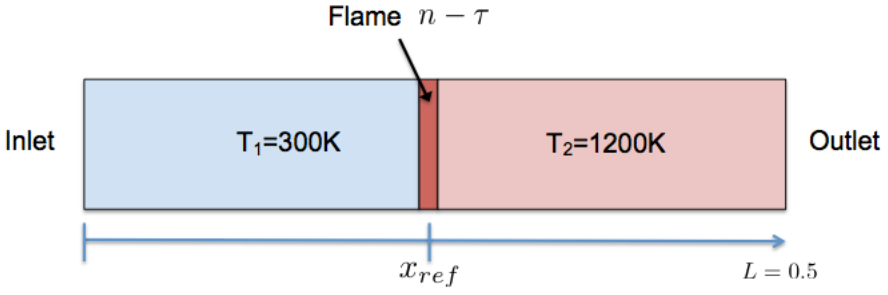

Figure 1: The configuration of the Rijke tube.

First, Eq. (6) is considered without a source term, which corresponds to the case of a passive flame with zero unsteady heat release. Then, the mean heat release is considered non- zero, which refers to an active flame case. The results of both the passive flame and the active flame are presented in Fig. 3.

Since the Neumann and the Dirichlet boundary conditions are applied at the inlet and outlet, respectively, the simple form of the dispersion relation could be obtained as Eq. (10) as the analytical solutions[9]. The eigenfrequencies of the Rijke tube are the solutions of the following dispersion relation as Eq. (10). In this section, the exact eigenfrequencies are compared to the numerical results obtained by the finite element method and the iterative algorithm.

$$cos\left(\frac{L}{4c_1}\omega\right)\left[cos^2\left(\frac{L}{4c_1}\omega\right)-\frac{1}{4}\frac{\Gamma(1+ne^{i\omega\Gamma})-1}{\Gamma(1+ne^{i\omega\Gamma})+1}-\frac{3}{4}\right]=0 \tag{10}$$

where the Γ is defined as the acoustic impedance ratio between the cool gas region and the hot gas region, which is formulated as:

$$\Gamma=\frac{\rho_2 c_2}{\rho_1 c_1} \tag{11}$$

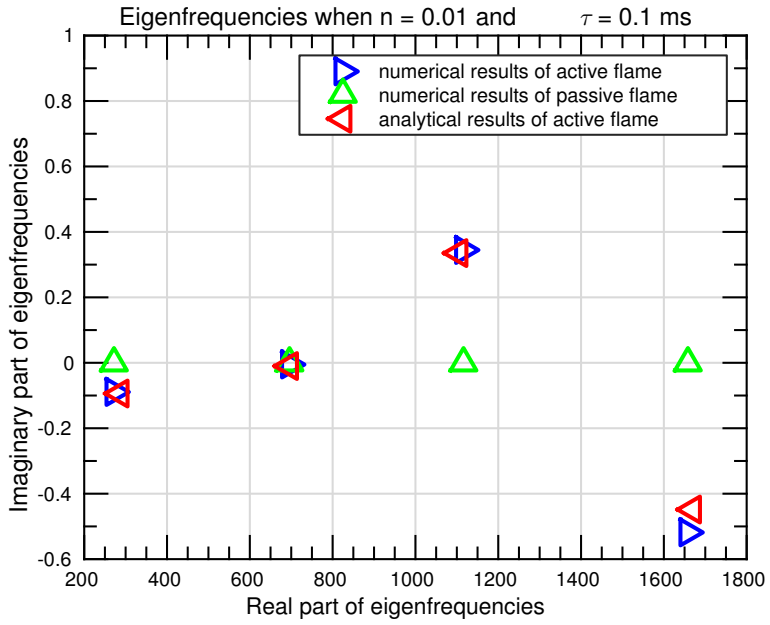

Figure 2: Comparison between the numerical results and the analytical results, passive flame case and active flame case are both included in the plot.

As shown in Fig. 3, the eigenfrequencies of the passive flame are purely real. Hence, the modes are neither amplified or damped. For the eigenfrequencies of the active flame, the numerical results are compared to the analytical results, which show that the first and the fourth modes are stable, and the third mode is unstable according to the positive growth rate.

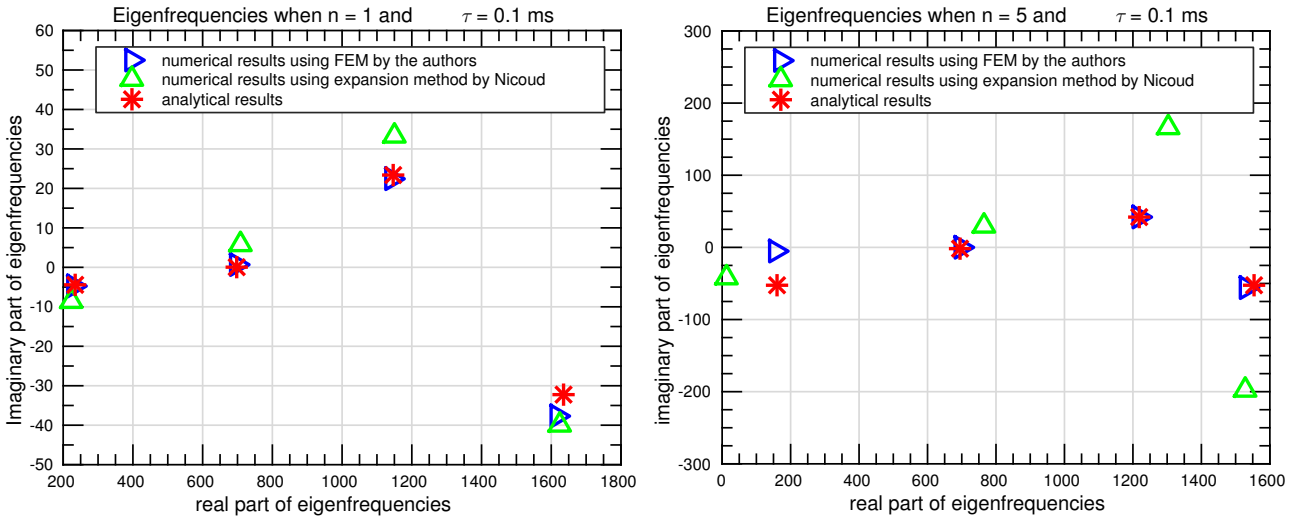

Figure 3: Numerical results using the FEM, the expansion method in [1] and analytical results from [9].

In Fig. 3. numerical results by using finite element method (FEM) and the expansion method by Nicoud [1] are compared to the analytical results of Eq. (10) from [9]. The numerical results obtained using FEM are in better agreement with the analytical results even when the flame interaction is strong ($n = 5$). It is also shown that the strength of the flame make a big impact on the instability of the system, the resonance frequency has been shifted around $180Hz$ at the fourth mode when n increases to 5.

About he mesh for the Rijke tube numerical case, which is around 16000 triangular cells are generated. The mesh is refined particular in the flame region.

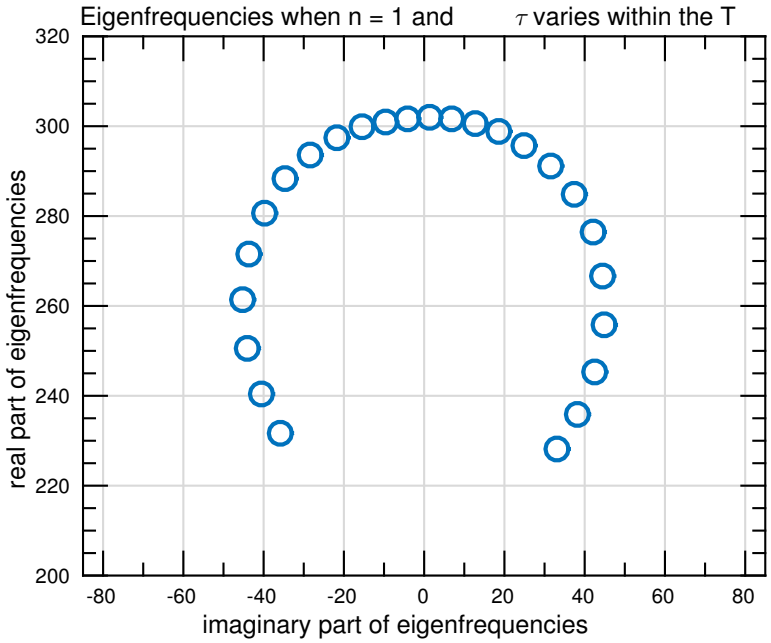

Figure 4: Plot of eigenfrequencies when $n = 1$ and the time lag τ takes the value from $\tau = 0$ to $\tau = 1/f_{1st}$ where $f_{1st} = 263Hz$.

In Fig. 4., the gain G ($G = n$ for the $n - \tau$ model) is held fix and τ is made to change from zero to $\tau = 1/f_{1st}$. This should lead to that the eigenfrequencies of the first mode should form a circle when plotted in the complex plane [7]. As can be seen, the results are validated since the center of

this circle is around (0 263), which is the eigenfrequency for the first mode of the passive flame case when $n = 1$.

With τ in the range of 0 to $\tau = 1/2f_{1st}$, the eigenfrequencies are located on the left half of the complex plane. The imaginary part of the eigenfrequency is always negative, which indicate that the system is stable. Meanwhile, the real part of the eigenfrequency, goes from a minimum to a maximum value. When the time lag is in the range between $1/(2f_{1st})$ and $1/f_{1st}$, the eigenfrequencies are located on the right half of the complex plane. The growth rate is positive and the system is unstable. The resonance frequencies change from a maximum to a minimum value. It can be concluded that the phase $\phi = 2\pi f_{1st}$ of the flame transfer function (FTF) defines whether the combustion system is stable or not.

However, when the time lag varies within one period, the plot of eigenfrequencies should exhibit as a complete circle. The discrepancies may be due to two numerical reasons: First, in the numerical simulations, the flame front can not be infinitely thin as in the analytical model. Since in the simulations, the flame thickness is at least as one cell of mesh. Second, the location of the reference point may also influences the numerical results. Since when the reference point is chosen, it is usually in the cool gas region or in the hot gas region, but not exactly located in the middle of the duct $x = L/2$, which of course leads to some discrepancies.

4. A V-flame within a dump combustor

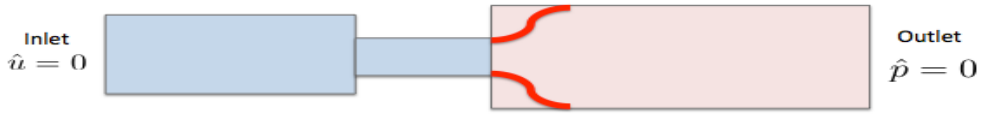

Figure 5: Simplified configuration for the V-flame numerical case.

In this section, the instability of a dump combustor with a V-flame is investigated numerically by solving the inhomogeneous Helmholtz in combination of the FTF. The dump combustor is represented by the numerical model illustrated in Fig. 5. as well as the boundary conditions. The temperature upstream of the flame is $300K$ and is $1600K$ downstream of the flame. The detailed dimensions of the numerical model can be found from the Ref. [7].

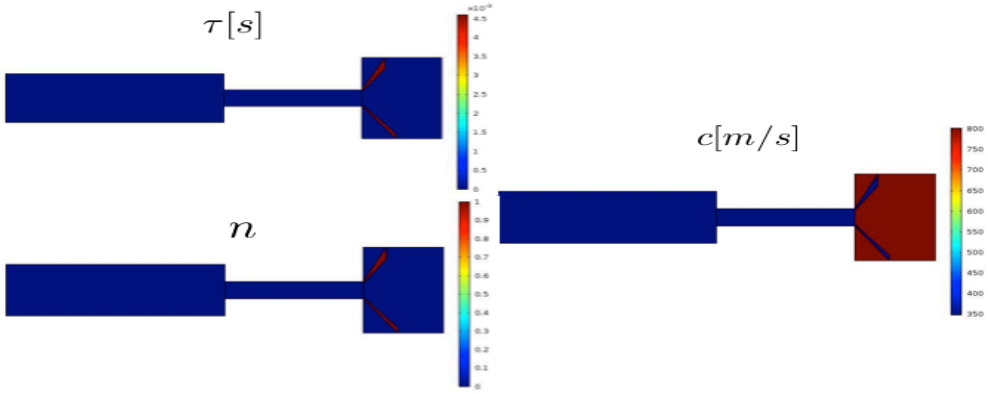

Figure 6: Fields needed for the simulations, upper is the time lag τ and lower is the sound speed c.

It the simulations, the time lag τ, the gain G and the speed of sound c are necessary for the computations. In Fig. 6, they are assumed that those quantities are non-zero in the flame region, but

zero else where. The sound speed has two different values in the whole computational domain due to the temperature difference before and after the flame. Hence, those variables are varying with the coordinates and are actually the most important factors influencing the instability of the system[7]. Furthermore, the shape of the V-flame (such as the thickness) and the position of flame (angle between the flame and the x-axis) are also key factors to the thermoacoustic instability. However, there is no enough information either for the shape of the V-flame or the position of the flame, those two variables are picked up by the authors currently.

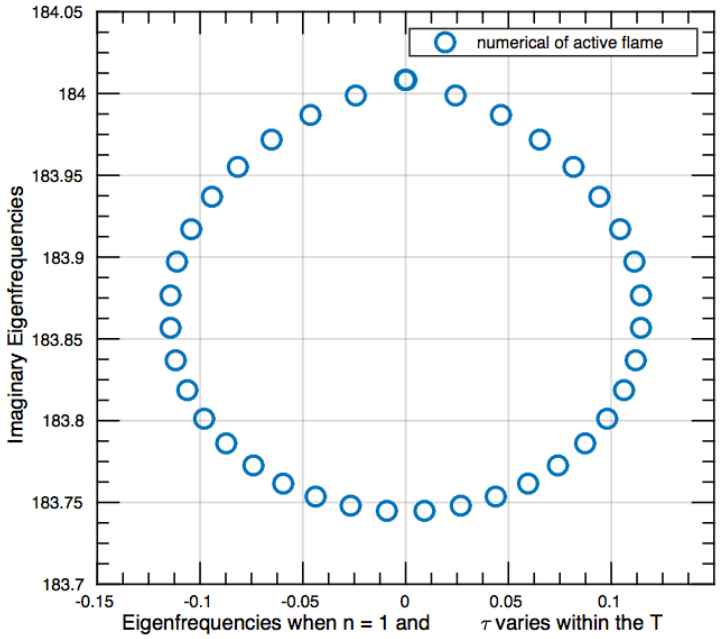

Figure 7: Plot of eigenfrequencies when n = 1 and the time lag τ takes the value from $\tau = 0$ to $tau = 1/f_{1st}$ where $f_{1st} = 183.90Hz$.

The eigenfrequencies plotted in Fig. 7. are distributed as a circle as well, which is consistent with the analytical solution, see [7]. It is shown that the time lag τ plays an important role and will determine the stability of the system. However, due to the lack of the information of the premixed flame, currently the the magnitude of the eigenfrequencies can not be compared with and verified with any measurements.

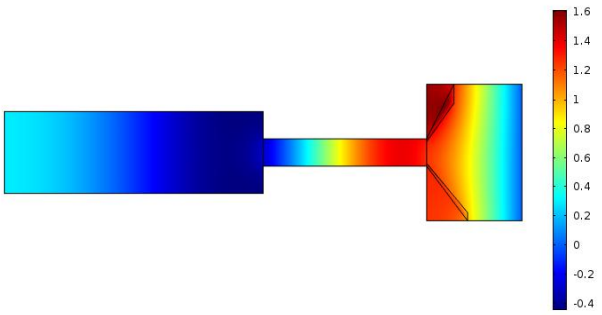

Figure 8: Contour plot of acoustic pressure for V-flame in a dump combustor when $G = 1$ and $\tau = 7.67 \cdot 10^{-4}s$ at the forth mode f=1885.7+4.5404i

Fig. 8. presents the forth acoustic mode when $G = 1$ and $\tau = 7.67 \cdot 10^{-4}s$. Since the size of the

numerical geometry is small, only the acoutic wave at higher frequency can be clearly shown. It can be seen that the in front of the flame region, the plane wave is propagating while after the flame, the wave is no longer the plane wave.

5. Conclusion

In the paper, a numerical methodology to predict the instability of a dumb combustor is presented. Specifically, an analytical flame model or flame transfer function is combined with the inhomogeneous Helmholtz equation, which is discretized using the Finite Element Method (FEM) and solved as a non-linear eigenvalue problem.

In this paper, the numerical solver has been validated for the Rijke tube case where the flame interaction index n and the time lag τ are varying. Then, the eigen frequencies and eigen vectors for a V-flame in the dump combustor has been simulated.

The results show that the Finite Element Method (FEM) gives excellent results when compared to theory.

Future work include numerical work to investigate the acoustic characteristics when V-flame.

Acknowledgement

The presented work is part of the Marie Curie Initial Training Network Thermo-acoustic and aero-acoustic nonlinearities in green combustors with orifice structures (TANGO). We gratefully acknowledge the financial support from the European Commission under call FP7-PEOPLE-ITN-2012. The simulations were performed at the facilities within the SNIC for high performance computing, KTH Stockholm.

References

1. Benoit, L. and Nicoud, F. Numerical assessment of thermo-acoustic instabilities in gas turbines, *International journal for numerical methods in fluids*, **47** (8-9), 849–855, (2005).

2. Baillot, F., Durox, D. and Prud'Homme, R. Experimental and theoretical study of a premixed vibrating flame, *Combustion and Flame*, **88** (2), 149–168, (1992).

3. Schuller, T., Durox, D. and Candel, S. A unified model for the prediction of laminar flame transfer functions: comparisons between conical and v-flame dynamics, *Combustion and Flame*, **134** (1), 21–34, (2003).

4. Lieuwen, T. and Zinn, B. T. The role of equivalence ratio oscillations in driving combustion instabilities in low no x gas turbines, *Symposium (International) on Combustion*, vol. 27, pp. 1809–1816, Elsevier, (1998).

5. Sattelmayer, T. Influence of the combustor aerodynamics on combustion instabilities from equivalence ratio fluctuations, *Journal of Engineering for Gas Turbines and Power*, **125** (1), 11–19, (2003).

6. Crocco, L. Aspects of combustion stability in liquid propellant rocket motors part i: fundamentals. low frequency instability with monopropellants, *Journal of the American Rocket Society*, **21** (6), 163–178, (1951).

7. Silva, C. F., Nicoud, F., Schuller, T., Durox, D. and Candel, S. Combining a helmholtz solver with the flame describing function to assess combustion instability in a premixed swirled combustor, *Combustion and Flame*, **160** (9), 1743–1754, (2013).

8. Nicoud, F., Benoit, L., Sensiau, C. and Poinsot, T. Acoustic modes in combustors with complex impedances and multidimensional active flames, *AIAA journal*, **45** (2), 426–441, (2007).

9. Nicoud, F. and Wieczorek, K. About the zero mach number assumption in the calculation of thermoacoustic instabilities, *International Journal of Spray and Combustion Dynamics*, **1** (1), 67–111, (2009).